Targeting NAD$^+$ salvage pathway induces autophagy in multiple myeloma cells via mTORC1 and extracellular signal-regulated kinase (ERK1/2) inhibition

*Michele Cea,[1,2] *Antonia Cagnetta,[1,3] Mariateresa Fulciniti,[1] Yu-Tzu Tai,[1] Teru Hideshima,[1] Dharminder Chauhan,[1] Aldo Roccaro,[1] Antonio Sacco,[1] Teresa Calimeri,[1] Francesca Cottini,[1] Jana Jakubikova,[1] Sun-Young Kong,[1,4] Franco Patrone,[2] Alessio Nencioni,[2] Marco Gobbi,[3] Paul Richardson,[1] Nikhil Munshi,[1] and Kenneth C. Anderson[1]

[1]LeBow Institute for Myeloma Therapeutics and Jerome Lipper Center for Multiple Myeloma Research, Dana-Farber Cancer Institute, Harvard Medical School, Boston, MA; Departments of [2]Internal Medicine and [3]Hematology and Oncology, Istituto Di Ricovero e Cura a Carattere Scientifico Azienda Ospedaliera Universitaria San Martino-IST, Genova, Italy; and [4]Research Institute and Hospital, National Cancer Center, Goyang, Korea

Malignant cells have a higher nicotinamide adenine dinucleotide (NAD$^+$) turnover rate than normal cells, making this biosynthetic pathway an attractive target for cancer treatment. Here we investigated the biologic role of a rate-limiting enzyme involved in NAD$^+$ synthesis, Nampt, in multiple myeloma (MM). Nampt-specific chemical inhibitor FK866 triggered cytotoxicity in MM cell lines and patient MM cells, but not normal donor as well as MM patients PBMCs. Importantly, FK866 in a dose-dependent fashion triggered cytotoxicity in MM cells resistant to conventional and novel anti-MM therapies and overcomes the protective effects of cytokines (IL-6, IGF-1) and bone marrow stromal cells. *Nampt* knockdown by RNAi confirmed its pivotal role in maintenance of both MM cell viability and intracellular NAD$^+$ stores. Interestingly, cytotoxicity of FK866 triggered autophagy, but not apoptosis. A transcriptional-dependent (TFEB) and independent (PI3K/mTORC1) activation of autophagy mediated FK866 MM cytotoxicity. Finally, FK866 demonstrated significant anti-MM activity in a xenograft-murine MM model, associated with down-regulation of ERK1/2 phosphorylation and proteolytic cleavage of LC3 in tumor cells. Our data therefore define a key role of Nampt in MM biology, providing the basis for a novel targeted therapeutic approach. (*Blood*. 2012;120(17):3519-3529)

Introduction

Multiple myeloma (MM) is a clonal B-cell malignancy characterized by excessive bone marrow plasma cells in association with monoclonal protein.[1] The therapeutics currently available improve patients' survival and quality of life, but resistance to therapy and disease progression remain unsolved issues. Therefore, the definition of new aspects of MM biology that can be targeted and exploited from a therapeutic perspective remains a major basic and clinical research goal.

Autophagy is a conserved process of normal cell turnover by regulating degradation of its components, which is characterized by the formation of autophagosomes, double-membrane cytoplasmic vesicles engulfing intracellular material including protein, lipids, as well as organelles, such as mitochondria and endoplasmic reticulum. Subsequently autophagosomes fuse with lysosomes, and their contents are degradated by lysosomal enzymes.[2] This self-cannibalization event is a highly conserved response to metabolic stress, in which cellular components are degraded for the maintenance of homeostasis.[3] Intriguingly, the waste removal function of autophagy appears as to be a double-edged sword, because it can either lead to cell survival or death.[4] A series of molecular mechanisms coordinate the autophagy machinery. Specifically, the mammalian target of rapamycin (mTOR) complex 1 (mTORC1) is the major intracellular hub for integrating autophagy-related signals.[5] Upstream of mTORC1 is the cellular energy-sensing pathway.[6] Regulation of autophagy also occurs through the transcription factors EB (TFEB) and forkhead box (FOXO), whose activation leads to transcription of Atg genes.[7,8] Although apoptosis induction has been the major focus of research in novel MM therapies, a recent study documented a pivotal role for autophagy as a prosurvival mechanism in MM cells, suggesting its potential as an additional target for novel therapeutics.[9,10]

Intracellular nicotinamide adenine nucleotide (NAD$^+$) plays a major role in the regulation of several cellular processes.[11,12] In mammals, NAD$^+$ is replenished from nicotinamide (Nam), tryptophan or nicotinic acid (NA), with Nam as the most important and widely available precursor.[13] Nicotinamide phosphoribosyltransferase (NAMPT), pre-B colony enhancing factor, is the rate-limiting enzyme in NAD$^+$ synthesis from Nam.[14] The expression of this enzyme is up-regulated in activated immune cells,[15] in differentiated myeloid cells,[16] during the circadian clock,[17] in glucose-restriction impaired skeletal myoblast differentiation,[18] and during cytokine production in immune cells.[19] Importantly, *Nampt* is also overexpressed in cancer cells, which exhibit a significant dependence on NAD$^+$ to support their rapid cell proliferation.[20] Importantly, a specific chemical inhibitor of Nampt FK866, also called APO866 or WK175, exhibits a broad antitumor activity both in vitro and in vivo against cell lines derived from several tumors, with a favorable therapeutic window.[21-24]

In this study, we show that Nampt inhibition induces a potent cytotoxic activity against MM cell lines and patient cells in vitro and in vivo, as well as overcomes the protection conferred by IL-6, IGF-1, or bone marrow stromal cells (BMSCs). This effect was

Submitted March 13, 2012; accepted August 19, 2012. Prepublished online as *Blood* First Edition paper, September 5, 2012; DOI 10.1182/blood-2012-03-416776.

*M.C. and A.C. contributed equally to this work.

The online version of this article contains a data supplement.

The publication costs of this article were defrayed in part by page charge payment. Therefore, and solely to indicate this fact, this article is hereby marked "advertisement" in accordance with 18 USC section 1734.

associated with inhibition of multiple downstream signaling cascades mediating MM cell growth and drug resistance. Moreover, using RNAi to knockdown *Nampt* we confirmed the key role of this enzyme in maintenance of both cellular viability and intracellular NAD^+ stores. Nampt inhibition triggered a marked increase in autophagy, evidenced by the presence of autophagic vacuoles in the cytoplasm, proteolytic cleavage of endogenous LC3-I to LC3-II, localization of GFP-LC3 in a punctata pattern, and transcription of several autophagy-related genes. This activation of autophagy by FK866 was because of both mTORC1/Akt and ERK1/2 pathway inhibition. First, FK866 treatment of MM cells induced autophagy by dual inactivation of mTORC1 and Akt. Second, inhibition of mitogen-activated protein kinase signaling (MAPK) resulted in nuclear localization of transcription factor EB, thereby leading to up-regulation of several autophagy-related genes independently of mTORC1. Taken together, our findings suggest the pivotal role of Nampt in MM cell growth, survival, and drug resistance, providing the framework for novel targeted therapy in MM.

Methods

For a more detailed description of the methods used, see supplemental Methods (available on the *Blood* Web site; see the Supplemental Materials link at the top of the online article).

Reagents

The Nampt inhibitor FK866 was generously provided by the National Institute of Mental Health (NIMH) Chemical Synthesis and Drug Supply Program. It was dissolved in dimethyl sulphoxide at 10mM and stored at −80°C for in vitro study. For in vivo studies in mice, FK866 was formulated in 0.9% saline solution and stored at −20°C. Autophagy inhibitors (3-methyladenine, wortmannin, LY294002, bafilomycin A1) and nicotinamide were purchased from Sigma-Aldrich. MEK 1/2 inhibitors (U0126 and AS703026) were obtained from Cell Signaling and EMD Serono, respectively. JNK inhibitor II and SB203580 (p38 MAPK inhibitor) were obtained from Calbiochem.

Cell lines and culture

Cell lines were obtained from the ATCC or were kindly provided by sources indicated in supplemental Methods. Samples were freshly isolated from bone marrow aspirates from patients. Further details are found in supplemental Methods.

Viability assay

Dead cells were quantified by propidium iodide (PI) staining (2 mg/mL) and flow cytometry (FACS Canto II; Becton Dickinson). Percentage of specific death was calculated as follows: $100 \times$ [experimental sample (%) − spontaneous sample (%) / 100 − spontaneous sample (%)].

Effect of FK866 on paracrine MM cell growth in the BM

MM1S cells (2×10^4 cells/well) were cultured for 72 and 96 hours in BMSC-coated 96-well plates (Corning Life Sciences) in the presence or absence of drug. DNA synthesis was measured by (^{3}H)–thymidine (Perkin-Elmer Life and Analytic Sciences) uptake, with (^{3}H)–thymidine added (0.5 μCi/well) during the last 8 hours of cultures.

Characterization of cell death

Cells were cultured with FK866 (0.1nM-33nM) for 96 hours. For caspase inhibition assays, cells were pretreated with pan caspase inhibitor (zVAD-fmk), caspase 3-(zDEVD-fmk) and caspase 9-(zLEHD-fmk) inhibitors (Calbiochem) for at least 2 hours before addition of FK866. For inhibition of autophagy, cells were incubated with the inhibitors wortmannin (0.25μM), LY294002 (5μM), 3-methyladenine (3MA 100μM), and chloroquine (20μM) for at least 30 minutes before FK866 treatment. Apoptosis was quantitated using annexin-V–FITC (BD Bioscience) staining and flow cytometric analysis, according to the manufacturer's protocol.

Determination of the intracellular NAD^+ levels

The intracellular content of NAD^+ was assessed with a sensitive enzyme cyclic assay (BioVision), according to the manufacturer's procedure. The value was normalized to protein concentrations (Micro-BCA kit; Pierce) or total cell number.

Stable gene knockdown using lentiviral vectors

To knockdown *Nampt* in MM cells, we used short hairpin RNA (shRNA) sequences and a lentivirus transfection system. The shRNAs were provided by Dr Anna Schinzel (Dana-Farber Cancer Institute). The sequences of the *Nampt* shRNA constructs were as follows: clone No. 1: 5′-GTAACT-TAGATGGTCTGGAAT-3′; clone No. 2: 5′-CCACCTTATCTTAGAGT-TATT-3′; clone No. 3: 5′-CCTACAAGGTTACTCACTATA-3′; clone No. 4: 5′-GAAGCCAAAGATGTCTACAAA-3′; and clone No. 5: 5′-CCACTAATAATCAGACCTGAT-3′. Briefly, pLKO.1 plasmid with *Nampt* shRNA or pLKO.1 control plasmid were cotransfected with packaging plasmid (pVSV-G and δ 8.9) into 293T cells with FUGENE 6 transfection reagent (Roche). Forty-eight and 72 hours after transfection, supernatant containing lentivirus particles was harvested, filtered, and used to infect (1×10^6 per mL) MM cells (RPMI8226/S, MM1S, and U266) with 8 μg/mL polybrene. Nampt protein expression and NAD^+ level were assayed 4 and 5 days after infection, respectively. The viability of MM cells after *Nampt* knockdown was analyzed by MTT and PI assays.

Immunoblotting

MM cells were cultured with or without FK866, harvested, washed, and lysed using radioimmunoprecipitation assay buffer, 2mM Na3VO4, 5mM NaF, and 1mM phenylmethylsulfonyl fluoride (5 mg/mL). Cell lysates were immediately boiled at 100°C for 10 minutes, and then stored at −20°C for subsequent use. Proteins were separated on an SDS-polyacrylamide gel and electroblotted on a polyvinylidene difluoride (PVDF) membrane (Pall Gelman Laboratory). Proteins were visualized by probing the membranes with the following antibodies: anti-mTOR, pospho(p)-mTOR (Ser2481), p70S6, pospho(p)-p70S6 (Thr421/Ser424), AKT, phospho(p)-AKT (Ser473), ERK1/2, P-ERK1/2, p38MAPK, P-p38MAPK (Thr180/Tyr182), P-SAPK/JNK (Thr183/Tyr185), SMAC/DIABLO, cytochrome-c, caspase-3, caspase-8, caspase-9, PARP, actin, as well as anti-LC3 and Beclin-1 antibodies (Cell Signaling Technology); anti-Nampt (Bethyl Laboratories); anti-JNK1, glyceraldehyde 3-phosphate dehydrogenase (GAPDH), nucleolin and γ-tubulin (Santa Cruz Biotechnology); and anti-DKK tag monoclonal Ab (Origene). Standard enhanced chemiluminescence was used for protein band detection.

Immunofluorescence

U266 and RPMI8226/S cells were transiently transfected with pEGFP-LC3B (Addgene), and treated with either vehicle or FK866 10nM for 24 and 48 hours. The GFP fluorescence was recorded using a Nikon E800 epifluorescence microscope equipped with a Coolsnap CF color camera (Nikon). For quantification, 10 fields, each consisting of 40-100 GFP-positive cells, were used to calculate the number of cells with GFP-LC3B puncta relative to the total number of GFP-positive cells.

Murine xenograft model of human MM

CB17-SCID mice (28-35 days old) were purchased from Charles River Laboratories. All animal studies were conducted according to protocols

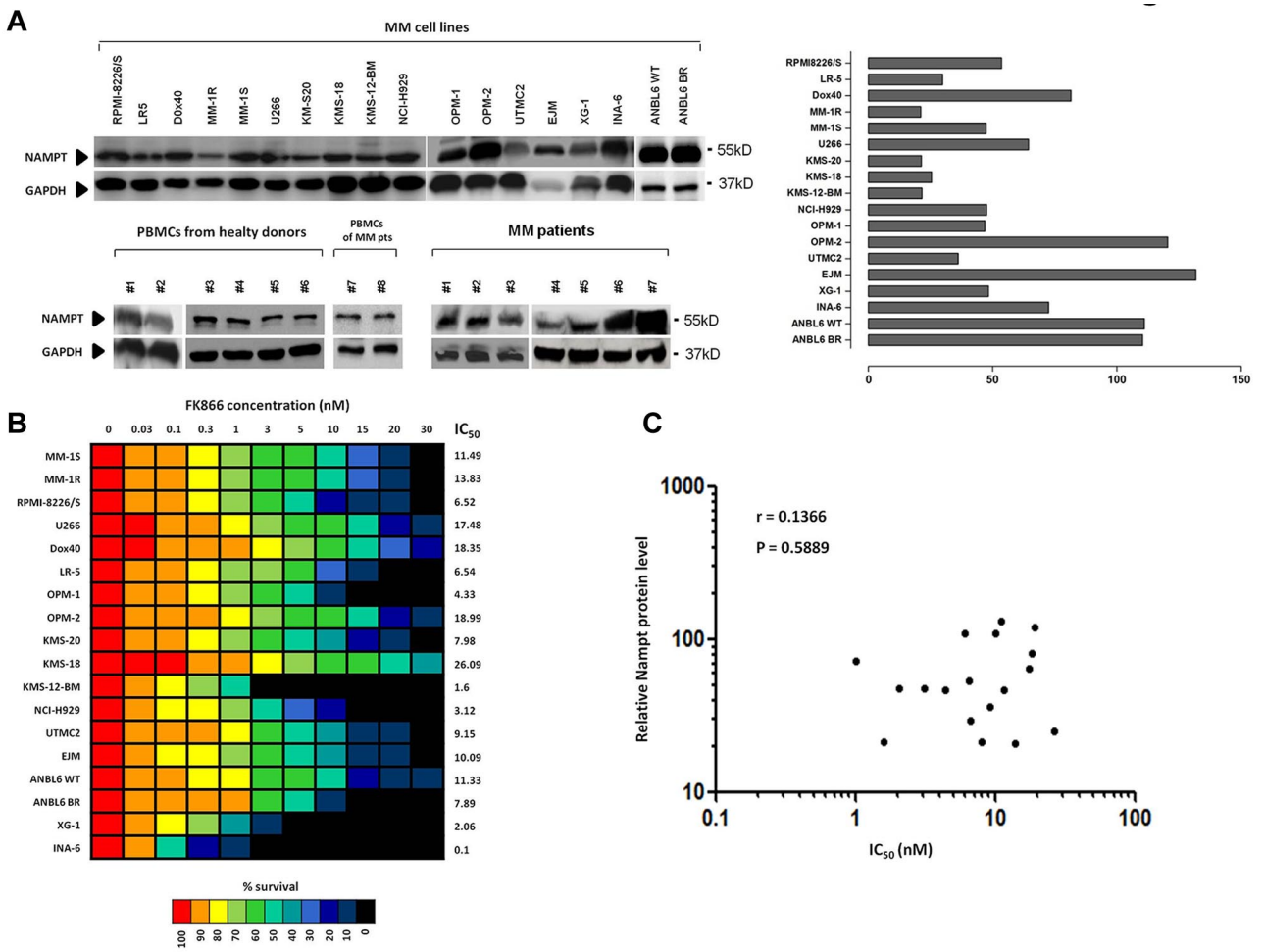

Figure 1. Nampt as therapeutic target in MM cells. (A) Expression of Nampt in multiple myeloma (MM) cell lines, patient MM CD138$^+$ cells, and peripheral blood mononuclear cells (PBMCs) from healthy donors or MM patients. Whole-cell lysates were subjected to immunoblotting with anti-Nampt antibody. Anti-GAPDH monoclonal antibody served as a loading control. Relative expression in MM cell lines was calculated as the ratio of the densitometry signal for Nampt relative to GAPDH in each sample using ImageJ Version 1.37 software (National Institutes of Health, http://rsb.info.nih.gov/ij/). (B) Dose-response effect in 18 human MM cell lines treated with FK866 (0-30nM for 96 hours). The percentage survival (expressed as percentage of the vehicle-treated control) is visualized in color format according to their values on a linear scale (0%-100%). Data presented are means ± SD of 3 experiments. (C) Relative expression of Nampt protein plotted versus 96h Fk866 cytotoxicity IC_{50} values. The Pearson correlation coefficient (r) and the *P* value, calculated using GraphPad Prism Version 5 analysis software are indicated.

approved by the Animal Ethics Committee of the Dana-Farber Cancer Institute. Mice were irradiated (200 cGy), and then inoculated subcutaneously in the right flank with 3×10^6 MM1S cells in 100 μL RPMI 1640. After detection of tumor (~ 2 weeks after the injection), 7 mice were treated intraperitoneally with either vehicle or FK866 (30 mg/kg body weight) twice a day for 4 days, repeated weekly over 3 weeks. Caliper measurements of the longest perpendicular tumor diameters were performed twice a week to estimate the tumor volume using the following formula: length × width^2 × 0.5. Tumor growth inhibition (TGI) was calculated using the formula (Δcontrol average volume − Δ treated average volume) × 100 (Δcontrol average volume). Animals were killed when tumors reached 2 cm^3 or the mice appeared moribund. Survival was evaluated from the first day of treatment until death. The images were captured with a Canon IXY digital 700 camera. Excised tumors from mice were collected and assessed by Western blotting.

Statistical analysis

Statistical significance of differences observed (in vitro and in vivo experiments) in drug-treated versus control was determined by Student *t* test; differences were considered significant when $P \leq .05$. Tumor growth inhibition and Kaplan-Meier survival analysis were determined using GraphPad Prism Version 5 analysis software.

Results

Nampt as therapeutic target in MM cells

We first evaluated the protein level of Nampt in MM by Western blot analysis. For this purpose we screened 18 MM cell lines, including those resistant to novel (ANBL6-BR) and conventional (MM.1R, LR-5, Dox40) therapeutic agents, observing expression of this protein in all cell lines tested (Figure 1A). Nampt protein was also detected in patient CD138+ MM cells (n = 7) and in PBMCs from healthy donors (n = 6) or MM patients (n = 2), with tumor cells exhibiting weakly higher levels compared with normal cells. This finding suggested that Nampt activity may be especially required for MM cell growth and function.

To address this hypothesis, we evaluated the antiproliferative activity of the chemical Nampt inhibitor FK866 against a panel of 18 MM cell lines and patient MM cells. As shown in Figure 1B, their viability was uniformly inhibited, with IC_{50} values at 96 hours ranging from 3 to 30nM. Notably and consistent with published data,[24] FK866 inhibited the growth of MM cells in a time and

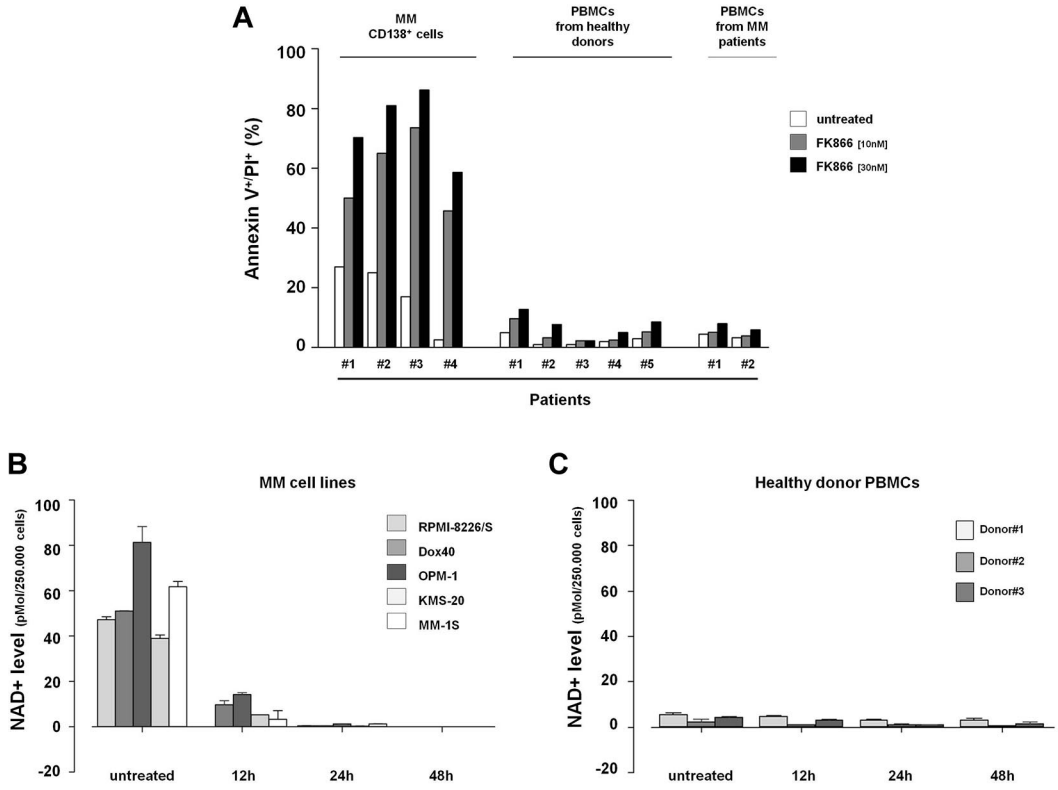

Figure 2. Nampt inhibition with FK866 induces significant NAD$^+$ intracellular reduction and selectively kills MM cells. (A) FK866 cytotoxic effect in primary cells. Purified patient MM cells (CD138$^+$) and PBMCs from healthy donors or MM patients were plated in 6-well plates and treated with FK866 at 10 and 30nM concentrations. After 72 hours (CD138$^+$ cells) or 96 hours (PBMC cells) were stained with fluorescein isothiocyanate (FITC)–conjugated annexin-V and PI, and analyzed by flow cytometry. (B-C) MM cell lines (B) and healthy donor PBMCs (C) were plated with or without FK866 10nM for the indicated times. Cells were harvested, and intracellular NAD$^+$ level was measured using an enzyme cyclic assay. The intracellular NAD$^+$ level was normalized relative to total cell number. Data presented are mean ± SD of 2 independent experiments.

dose-dependent manner (supplemental Figure 1A). In addition, Nampt inhibition also killed MM cell lines resistant to anti-MM agents including dexamethasone-resistant MM.1R, doxorubicin-resistant Dox40, melphalan-resistant LR5, and bortezomib-resistant ANBL-6BR cells. The antiproliferative effect of FK866 in MM cells was further confirmed by (^{3}H)–thymidine uptake assay (supplemental Figure 1B) To determine whether Nampt protein level correlates with efficacy of FK866 treatment, we compared the protein levels with IC_{50} values for all the MM cells tested, but the correlation (Pearson value .1366) was not significant (Figure 1C; $P = .5889$). These results suggest that Nampt protein level is not predictive of FK866 activity in MM cells.

FK866 also significantly reduced viability of CD138$^+$ patient-MM cells (n = 4) sparing PBMCs from 5 healthy volunteers. Importantly, although we previously reported an increased susceptibility to NAD$^+$ lowering drug of PBMCs activated,[25,26] mononuclear cells from MM patients were mostly unaffected. Collectively these data indicate that the anti-MM effect of FK866 is not because of a nonspecific effect on all hematopoietic cells resulting in a favorable therapeutic index in MM patients (Figure 2A).

MM cells undergo significant NAD$^+$ reduction after Nampt inhibition/depletion

Because treatment with Nampt inhibitor induces a significant reduction of intracellular NAD$^+$ levels, we hypothesized that the increased toxicity of FK866 in MM cell lines compared with healthy PBMCs was because of a differential response in intracellular levels of NAD$^+$. Using a cycling enzymatic assay, we observed that FK866 treatment dramatically reduced intracellular NAD$^+$ to undetectable levels in MM cell lines. In time-course experiments where intracellular NAD$^+$ level was monitored in cells treated with FK866 10nM, a significant NAD$^+$ decrease was detected as early as 12 hours in MM cells (Figure 2B) but not in healthy PBMCs (Figure 2C). FK866 treatment depleted cellular NAD$^+$ content selectively in MM cells, without a concomitant decrease of Nampt protein level (supplemental Figure 1C). Therefore, FK866-induced cell death is associated with inhibition of Nampt activity, rather than protein expression, and higher NAD$^+$ baseline levels in MM cells than normal PBMCs confer FK866 sensitivity. This effect of Nampt inhibition can be rescued by repletion of NAD$^+$ through biosynthesis from nicotinamide (Nam),[21] and we consistently found that exogenous Nam fully reversed FK866-induced MM cell death, further confirming that the effect of FK866 is because of NAD$^+$-depletion (supplemental Figure 2A).

To further investigate the role of Nampt in MM cell biology, we next evaluated the effect of *Nampt* knockdown on MM cell survival and intracellular NAD$^+$ level. Using 5 different shRNAs targeting *Nampt* in a lentivirally delivered arrayed shRNA screen, we found that reduction of Nampt levels was associated with both RPMI-8226/S cell death and intracellular NAD$^+$-depletion. (Figure 3A-C) Specifically, the most effective gene knockdown (shRNA no. 1, no. 3, and no. 4) was associated with higher MM cell death and depletion of intracellular NAD$^+$ compared with vector control shRNA. Conversely, shRNAs no. 2 and no. 5, without efficient knockdown, did not alter viability or NAD$^+$ intracellular level, further confirming the specificity of the effect. To assess the

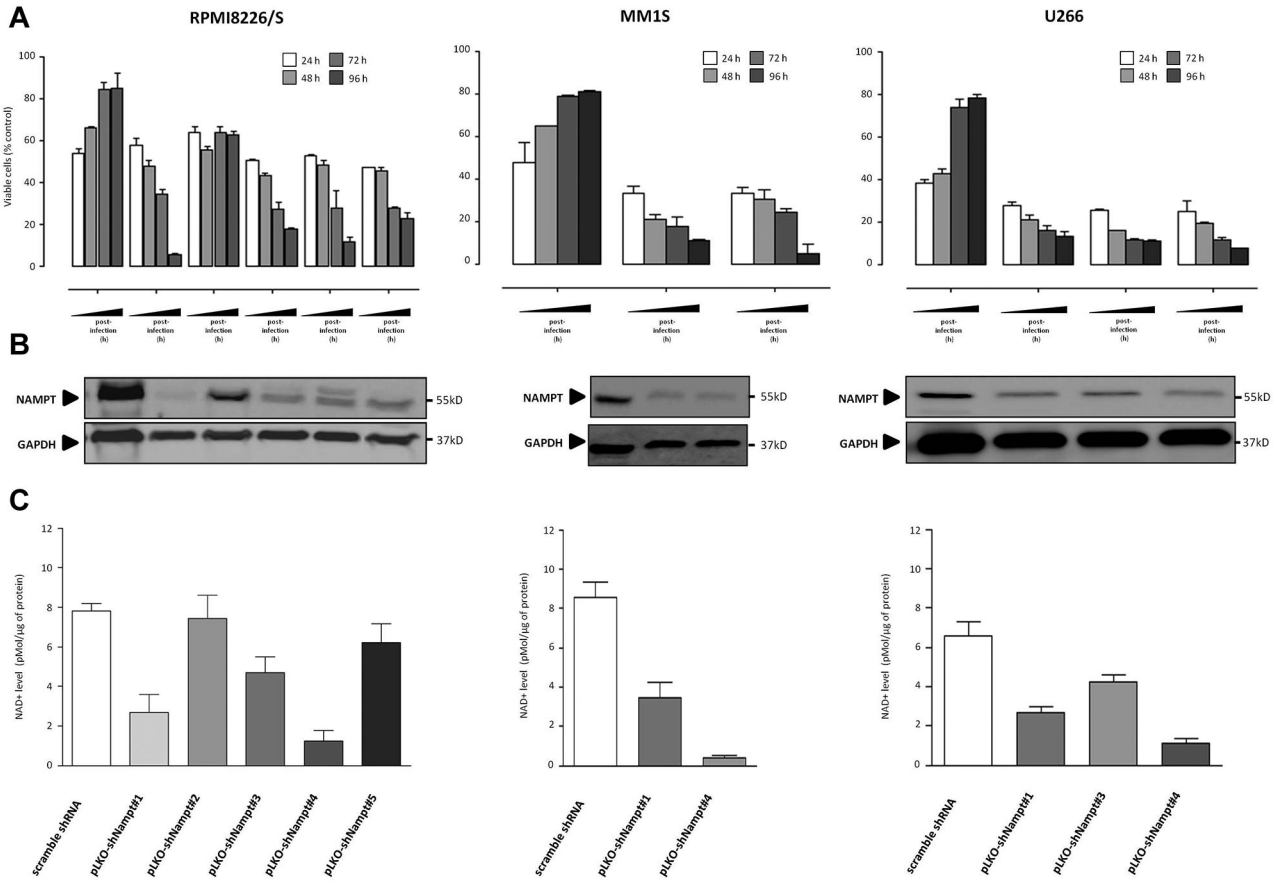

Figure 3. Effect of *Nampt* stable knockdown on MM cells. (A) RPMI-8226/S, MM-1S, and U266 cells were infected with either control scrambled or 5 independent lentiviral constructs expressing shRNAs targeting *Nampt* (RPMI8226/S: no. 1, no. 2, no. 3, no. 4, and no. 5; MM1S: no. 1 and no. 4; U266: no. 1, no. 3, and no. 4). The effect of *Nampt* knockdown on cell viability was assessed by MTT analysis and presented as the percentage of control cells. Data represent mean ± SD of 2 independent experiments carried out in triplicate. (B) Four days after infection, cell lysates were subjected to Western blot analysis to assess Nampt protein expression. (C) The effect of *Nampt* knockdown on intracellular NAD^+ level in MM cells infected with shRNAs (scramble or targeting Nampt) was assessed by enzyme cyclic assay and normalized to protein concentrations. Cells were analyzed 5 days after transduction.

breadth of these findings in MM, we confirmed similar shRNA-related results in MM cell lines with different genetic background (MM1S and U266). Taken together, these data confirm the pivotal role of Nampt in MM cell growth and survival.

FK866 abrogates the survival advantage conferred by the BM microenvironment

Because interaction of MM cells with BMSCs confers resistance to numerous therapeutic agents,[27,28] we first evaluated the expression of Nampt transcript in MM cells binding to BMSCs by analysis of published gene expression datasets.[28] Interestingly, *Nampt* was markedly up-regulated at mRNA level in MM cell lines (MM1S, MM1R, and INA6) on binding to bone stromal cells (Figure 4A; $P = .0025$, .0012, and .0006), supporting its biologic role in promoting MM cell growth within the BM microenvironment.

In such a scenario we next characterized the effect of the BM milieu on MM sensitivity to FK866. MM1S cells were incubated with IL-6 (10 ng/mL) or IGF-1 (100 ng/mL) or cocultured with BMSCs, and then treated with increasing doses of FK866 for 72 hours; proliferation was measured by thymidine uptake assay. As shown in Figure 4B and C, FK866 completely overcomes the protective effects of IL-6 and IGF-1, as well as coculture with BMSCs. Remarkably, no significant growth inhibition in BMSCs was measured. Thus FK866 preserves its anti-MM activity even in the context of the BM microenvironment.

Nampt inhibition induces autophagic MM cell death

To define the mechanism of FK866-mediated MM cell death, we first examined apoptosis and used the pan-caspase inhibitor zVAD-fmk as well as specific inhibitors of caspase 3 and 9 before treatment with FK866. As shown in supplemental Figure 3A, these inhibitors failed to protect from FK866-induced MM cell death. Moreover, we did not detect PARP or caspase-3, 8, and 9 cleavage triggered by FK866 (supplemental Figure 3B). These data rule out apoptosis as a mechanism whereby Nampt inhibition exerts its anti-MM activity. The integrity of mitochondrial transmembrane was next measured using tetramethylrhodamine ethyl ester (TMRE) cell staining. As shown in supplemental Figure 2B and C, FK866 treatment induced decreased mitochondrial transmembrane potential ($\Delta_{\psi m}$) accompanied by cytochrome c release in the cytosolic fraction. Because previous studies linked NAD^+ synthesis inhibition to the induction of autophagy in leukemia and neuroblastoma cells,[24,29] we next examined whether FK866 treatment also triggers autophagy in MM cells. Initially we used a chemical approach with PI3K inhibitors (3-methyl adenine, LY294002, and wortmannin) and the lysosomotropic drug chloroquine in combination with FK866 treatment. As predicted, all these autophagy modulators significantly reduced FK866-induced MM cell death (supplemental Figure 3C), confirming autophagy in response to this drug.

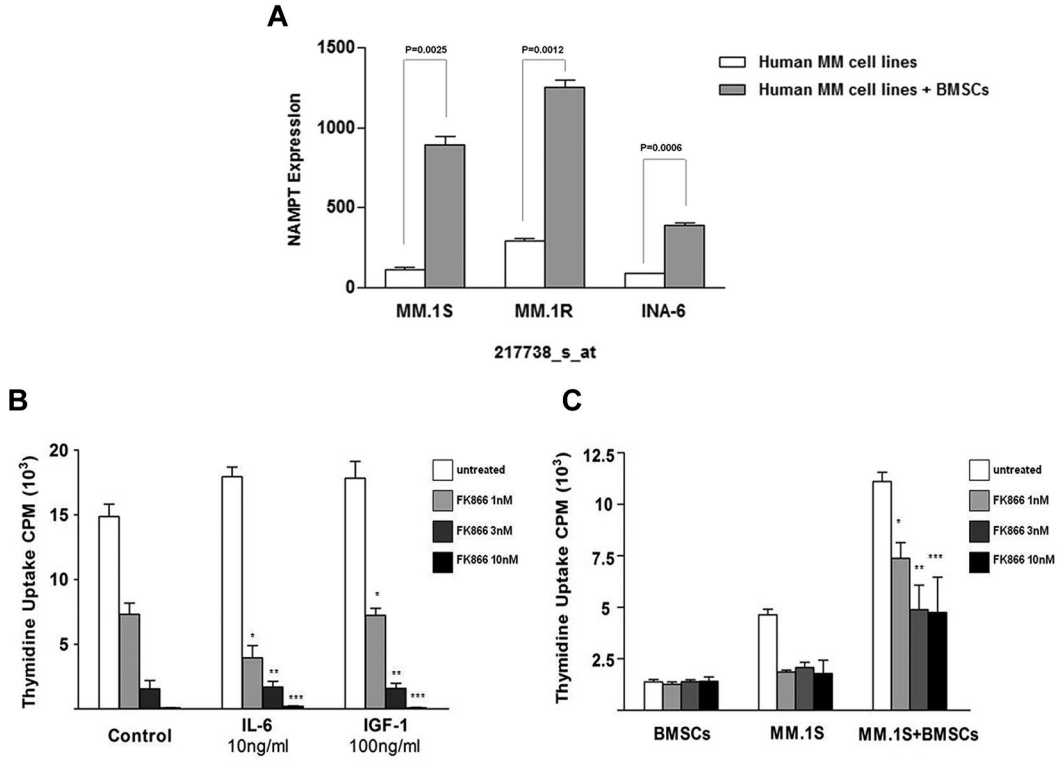

Figure 4. FK866 abrogates the survival advantage conferred by the bone marrow microenvironment. (A) Expression levels (linear scale) for Nampt transcripts were evaluated using oligonucleotide microarray data for MM1S, MM1R, and INA6 cells cultured in vitro in the presence or absence of HS-5 bone marrow stromal cells (GSE 20 540). (B) MM-1S cells were treated with FK866 (1-10nM) in the presence or absence of rhIL-6 (10 ng/mL) or rhIGF-1 (100 ng/mL) for 72 hours, and DNA synthesis was determined by (^{3}H)-thymidine uptake. The results presented are a mean ± SD of triplicate samples (*/**/***; $P < .0001$). (C) MM-1S cells were treated with FK866 (1-10nM) in the presence or absence of BMSCs for 72 hours, followed by measurements of proliferation using (^{3}H)–thymidine incorporation assay. Data presented are means ± SD of triplicate samples (*$P = .0019$; **$P = .0010$;***$P = .0034$).

To further support this notion, we investigated the morphologic characteristics of FK866-induced cell death using electron microscopy (EM). Three MM cell lines (MM.1S, U266, and RPMI-8226/S) were culture for 24 and 48 hours in the absence or presence of 10nM FK866, and then subjected to EM. In FK866-treated cells (Figure 5A high power view), vacuoles surrounded by a double-membrane characteristic of autophagosomes appeared at 24 hours after treatment, which contained endoplasmic reticulum and cytoplasm membrane fragments (arrows). Importantly, untreated cells lacked autophagosomes. At 48 hours treatment, the number of autophagosomal vacuoles markedly increased in all MM cells analyzed. To gain further insights into the role of autophagic process in FK866-induced MM cell death, we monitored the levels of LC3B-II, a lapidated form of microtubule-associated protein 1 light-chain 3 (LC3B) characteristic of autophagy, which can be detected by SDS-PAGE (LC3B-II).[30] Western blot analysis (Figure 5B) showed that FK866 treatment triggered a time-dependent detectable conversion from LC3-I to LC3B-II in U266 and MM1S cells. Quantification of the immunoblots revealed that treatment induced a 3-fold increase in LC3B-II levels in MM1S cells and 7-fold increase in U266 cells. Accumulation of Beclin-1, another marker of autophagy, was also rapidly induced in FK866-treated cells (Figure 5B). To confirm these results, we performed an additional experiment in which the frequency of cells displaying membrane translocation of the autophagosome component reporter LC3 was measured. RPMI8226/S and U266 cells were transiently transfected with a plasmid expressing a GFP-LC3B fusion protein.[30,31] Untreated cells showed GFP-LC3B to be uniformly distributed in the cytosol, whereas FK866, as well as rapamycin-treatment (a well-known inducer of autophagy) increased the formation of GFP-LC3B-labeled punctae, indicating autophagosome formation. (Figure 5C-D) To extend these results, we quantified GFP-LC3 punctae formation using a FACS-based assay.[32] As shown in Figure 5E, GFP-LC3 punctae were increased in FK866-treated cells versus control, indicating that treatment enhanced autophagy in MM cells. Finally, gene expression profiling confirmed the role of autophagy in FK866-induced cell death, showing an increase ≥ 2-fold of several autophagy-related genes after 6 and 24 hours of treatment (Figure 6C). Collectively, our data therefore show that autophagy contributes to death in MM cells because of Nampt inhibition, associated with mitochondrial dysfunction but not with caspase activation.

FK866-induced autophagy involves PI3K/AKT/mTOR pathway

Signaling pathways linking growth factor receptors, PI3K, Akt, and mTOR are tightly regulated in cells and commonly activated in cancer.[33] In addition, mTOR signaling is implicated as a master negative-regulator of autophagy.[34] We therefore next examined whether FK866-induced autophagy involves this pathway by assessing its effects on phosphorylation of mTOR and its substrate p70S6K. Three different MM cell lines (MM1S, U266, and RPMI8226/S) were exposed to FK866 10nM for 24 to 48 hours. Figure 6A shows, as expected, that FK866 treatment inhibited mTOR signaling, evidenced by a consistent reduction in mTOR phosphorylation at 24 hours in all MM cells analyzed. These changes were paralleled by decreased in phosphorylation of downstream p70S6K, confirming that mTOR signaling mediates FK866-induced autophagy. Inhibition of mTOR signaling leads to activation of PI3K and Akt,[35] and a dual inhibitor of PI3K and mTOR can block this feedback activation.[36] Consistent with this data, treatment

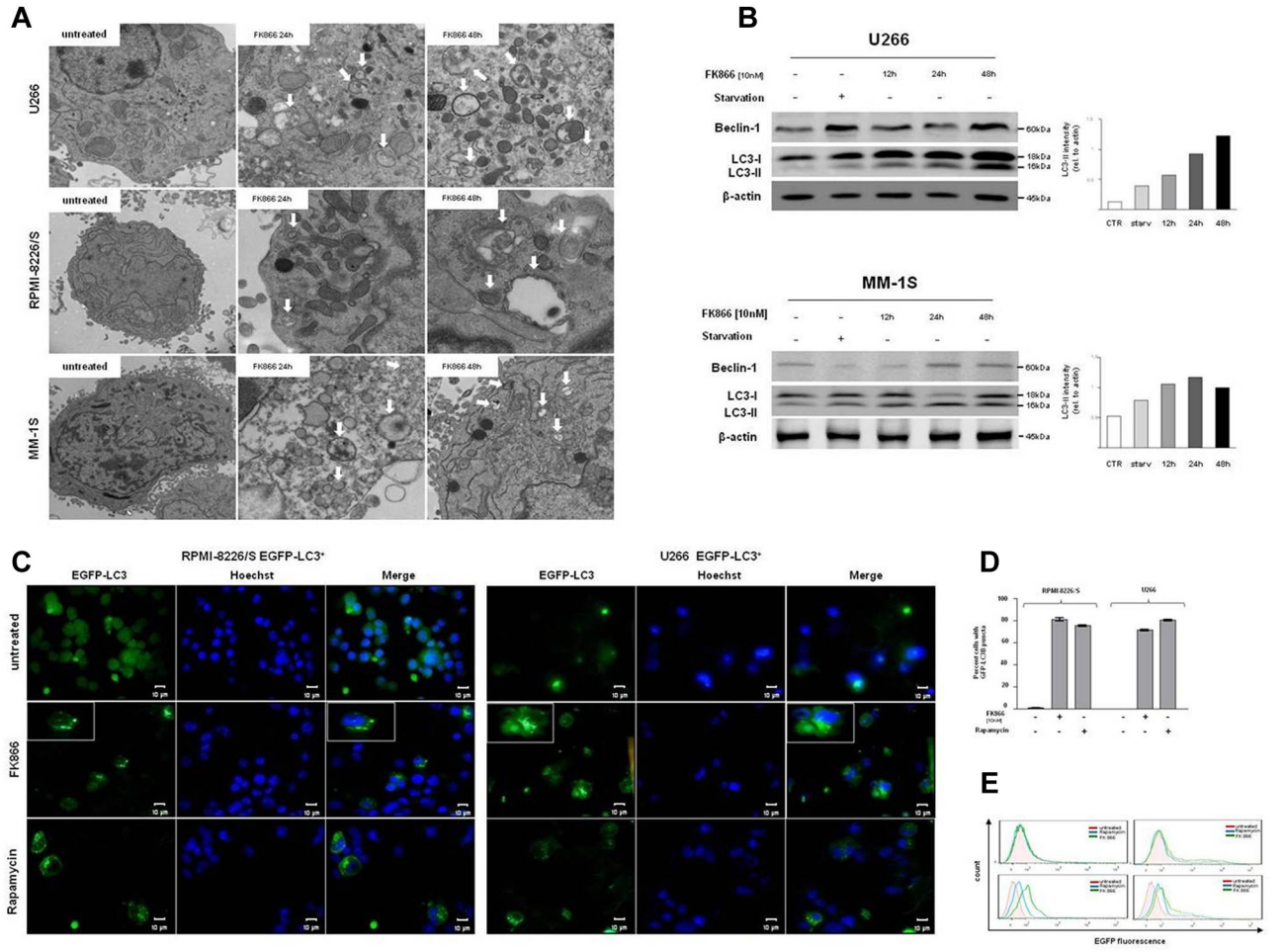

Figure 5. Nampt inhibition induces autophagic cell death of MM cells. (A) Electron microscopy of U266, RPMI-8226/S, and MM-1S cells treated with 10nM FK866 for 24 to 48 hours. Autophagic structures (autophagosomes) were observed on FK866 treatment as a double isolation membrane surrounding electron-dense cytoplasmatic material (arrows; direct magnification 2900× [untreated] and 9300 × [treated]). (B) Immunoblot analysis of LC3 and Beclin-1 protein levels in U266 and MM-1S cells treated with FK866 for indicated times or starved. Relative intensity of LC3 was calculated by normalizing the LC3-II intensity to β-actin using ImageJ Version 1.46 analysis software. (C) RPMI-8226/S and U266 cell lines were transfected with GFP-LC3 plasmid before treatment with FK866 or rapamycin (positive control). After 48 hours (FK866) or 24 hours (rapamycin), the autophagy flux was analyzed by immunofluorescence. Nuclei were counterstained with Hoechst. Fluorescence was recorded using a Nikon E800 epifluorescence microscope equipped with a Coolsnap CF color camera (Nikon; 40× magnification). Representative images from 2 independent experiments are shown for each point. (D) Quantification of percentage of GFP-LC3 puncta positive cells (mean ± SEM; n ≥ 50 cells per condition). (E) RPMI-8226/S-GFP-LC3$^+$ and U266-GFP-LC3$^+$cells were treated as described, washed briefly in 0.05% saponin in PBS or PBS alone, and then analyzed by flow cytometry for total GFP fluorescence. Data are representative of 2 independent experiments.

with FK866 was accompanied by an early (24 hours) increase of Akt phosphorylation at Ser^{473}, followed by a rapid decrease after 48 hours, in all MM cells tested. Moreover, these observed changes in Western blot were associated with gene expression level changes after FK866 treatment (10nM; 6 and 24 hours). Specifically, down-regulation of transcript levels of mTORC1/2 signaling genes confirmed suppression of this pathway by Nampt inhibitor. (Figure 6C) Thus dual inhibition of PI3K/mTOR (mTORC1/2) represents a crucial molecular event contributing to FK866-induced autophagy in MM cells.

MAPK pathway deregulation contributes to FK866-induced autophagy via TFEB nuclear mobilization in MM cells

The MEK/ERK pathway plays a pivotal role in promoting growth and survival of malignant B cells.[37] In addition, crosstalk between MEK/ERK and PI3K/Akt signaling pathways has been demonstrated in MM cells.[38] We therefore next examined the effects of Nampt inhibitor on MAPK signaling pathway in MM cells. Treatment of RPMI8226/S, U266, and MM1S cells with FK866 (10nM for 24-48 hours) significantly decreased both gene and protein levels of pERK1/2, pp38MAPK, and pSAPK/JNK confirming a potent inhibitory effect of this drug on MEK/ERK signaling (Figure 6B-D).

Recently, a novel transcriptional mechanism regulating the autophagic pathway has been identified.[7] Specifically, the transcription factor EB (TFEB), a master gene for lysosomal biogenesis, drives expression of a large subset of autophagy genes. Importantly, this transcription factor is kept inactive in the cytoplasm via a phosphorylation-dependent mechanism, and translocates to the nucleus when dephosphorylated. The cellular localization and activity of TFEB is regulated by a member of the mitogen-activated protein (MAP) kinase family, ERK2. During starvation, reduced phosphorylation by ERK2 leads to mobilization of TFEB into the nucleus and activation of a transcriptional program that increases autophagy. We therefore reasoned that the MAPK pathway-inhibitory effect induced by FK866 may contribute to autophagy triggered by this treatment. To test this mechanism, we ectopically expressed TFEB (DDK-TFEB) in U266 cells and then treated cells with FK866. Importantly, we used a sublethal dose of FK866 to ensure that

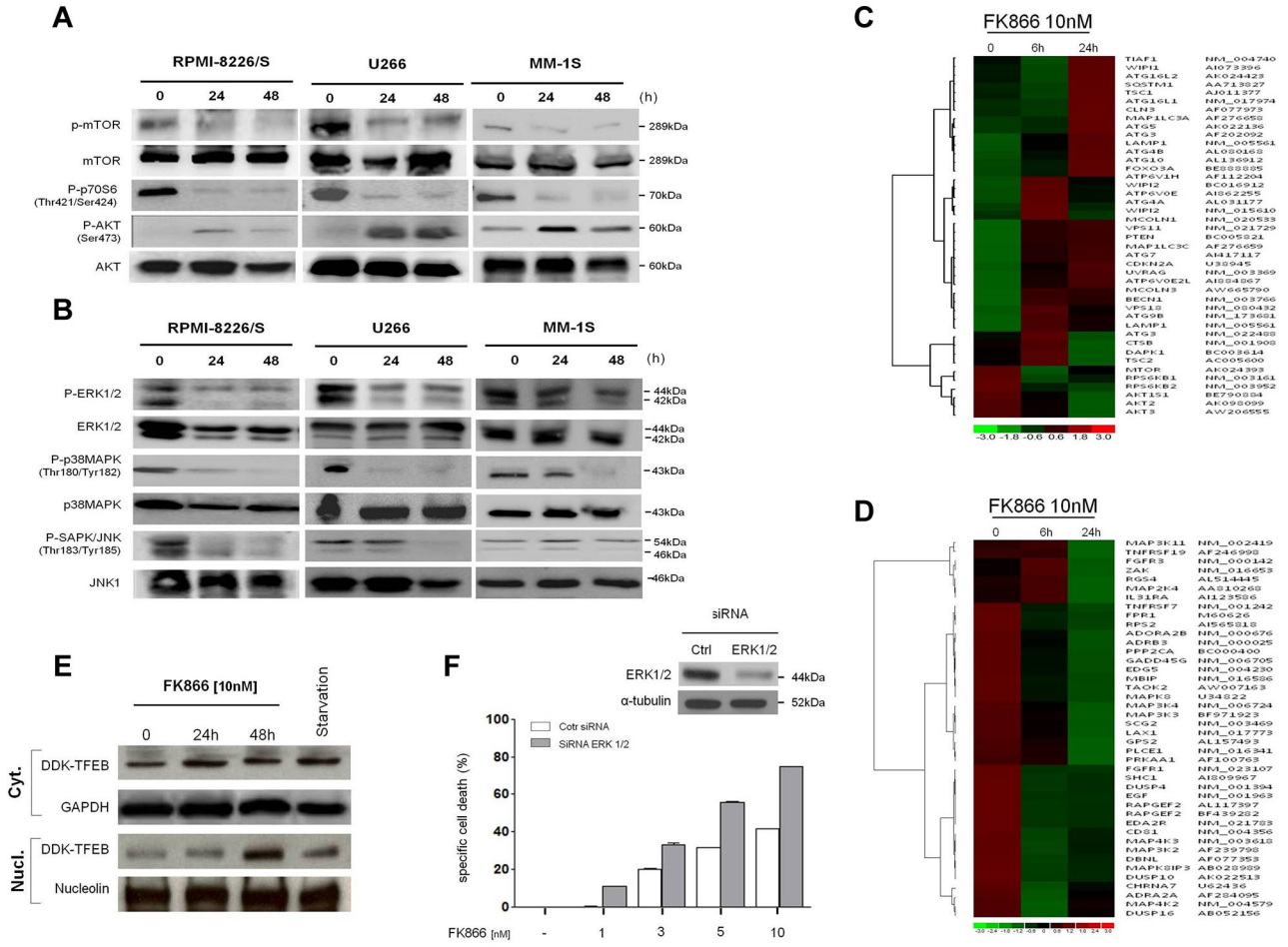

Figure 6. FK866 mediates autophagy by transcriptional-dependent and independent mechanisms. (A-B) RPMI-8226/S, MM-1S, and U266 cells were cultured with FK866 (0-10nM) for 24 to48 hours. Whole-cell lysates were subjected to immunoblotting using with the indicated antibodies. (C-D) Hierarchical clustering analysis of gene expression profiles of MM-1S cells treated with FK866 versus control. In panel C are shown autophagy-related genes (Pearson correlation 0.997 and 0.994 at 6 and 24 hours, respectively; $P < .0001$); in panel D MAPK-related genes (Pearson correlation .911 at 6 hours and .921 at 24 hours; $P < .0001$); fold change in the expression of FK866-treated cells relative to expression in untreated cells is shown by the intensity of induction (red) or suppression (green). The Gene expression data have been deposited in Gene Expression Omnibus (GEO; GSE35414) as reported in supplemental Methods. (E) U266 cells ectopically expressing a DDK-TFEB fusion protein were starved or treated with FK866 for 0 to 48 hours. Immunoblot analysis of DKK, GAPDH, and nucleolin was performed in nuclear/cytosolic extracts. (F) U266 cells were transfected with 200nM of siRNA ERK 1/2 or nontargeting siRNA. Two days later, cells were subjected to immunoblotting (top panel) or plated in 96-well plates and incubated with FK866 (0-10nM). The specific cell death was measured after 72 hours by PI staining and cytometry. A representative experiment is presented.

cell viability was not affected. As shown in Figure 6E, TFEB is normally localized to the cytoplasm, and treatment with FK866 induced TFEB nuclear translocation at 48 hours, as did serum starvation. Additional confirmation of the pivotal role of MAPK pathway in FK866-induced cell death was demonstrated by pretreatment of U266 cells with 3 different MEK/ERK biochemical inhibitors (U0126, SB203580, and AS703026), followed by FK866 (1-10nM) treatment. As shown in supplemental Figure 4A-C, FK866-induced cell death was synergistically increased in the presence of MAPK inhibitors. Notably, the involvement of ERK1/2 in FK866-induced cell death was also confirmed by using siRNA strategy. Blockade of ERK1/2 by siRNA also significantly enhanced FK866-induced MM cell death (Figure 6F). Consistent with these data, an overexpression of autophagic TFEB-target genes was observed in FK866-treated cells (supplemental Figure 4D). TFEB-nuclear mobilization therefore functionally contributes to FK866-induced autophagy in MM cells. Taken together, these data clearly demonstrate that MAPK-inhibition induced by FK866 contributes to autophagy triggered by this treatment.

In vivo anti-MM efficacy of FK866

To investigate whether Nampt inhibition by FK866 could inhibit MM cell growth in vivo, we used CB17-SCID mice xenografted subcutaneously with MM.1S cells. Fourteen tumor-bearing mice were randomly assigned to receive either 30 mg/kg of FK866 administered by intraperitoneal injection (twice a day for 4 days consecutively followed by 3 days off therapy in each cycle, repeated over 3 weeks) or vehicle control. Figure 7A shows the comparison of MM.1S growth in cohorts receiving vehicle control (n = 7) versus treatment (n = 7). A significantly decreased tumor burden was observed as early as day 7 of treatment and was confirmed at day 21, in treated compared with control mice. ($P = .0061$ and $P = .0067$, respectively). Importantly, the treatment was well tolerated, without significant weight loss or neurologic changes, and resulted in a significant prolongation in overall survival (Figure 7B; $P = .0014$). The median overall survival was 19.5 days in control group versus 45 days in the FK866-treated group. Tumors were harvested, and lysates were subjected to Western blot analysis to evaluate phosphorylation of ERK and LC3B (Figure 7C). Consistent with our in vitro

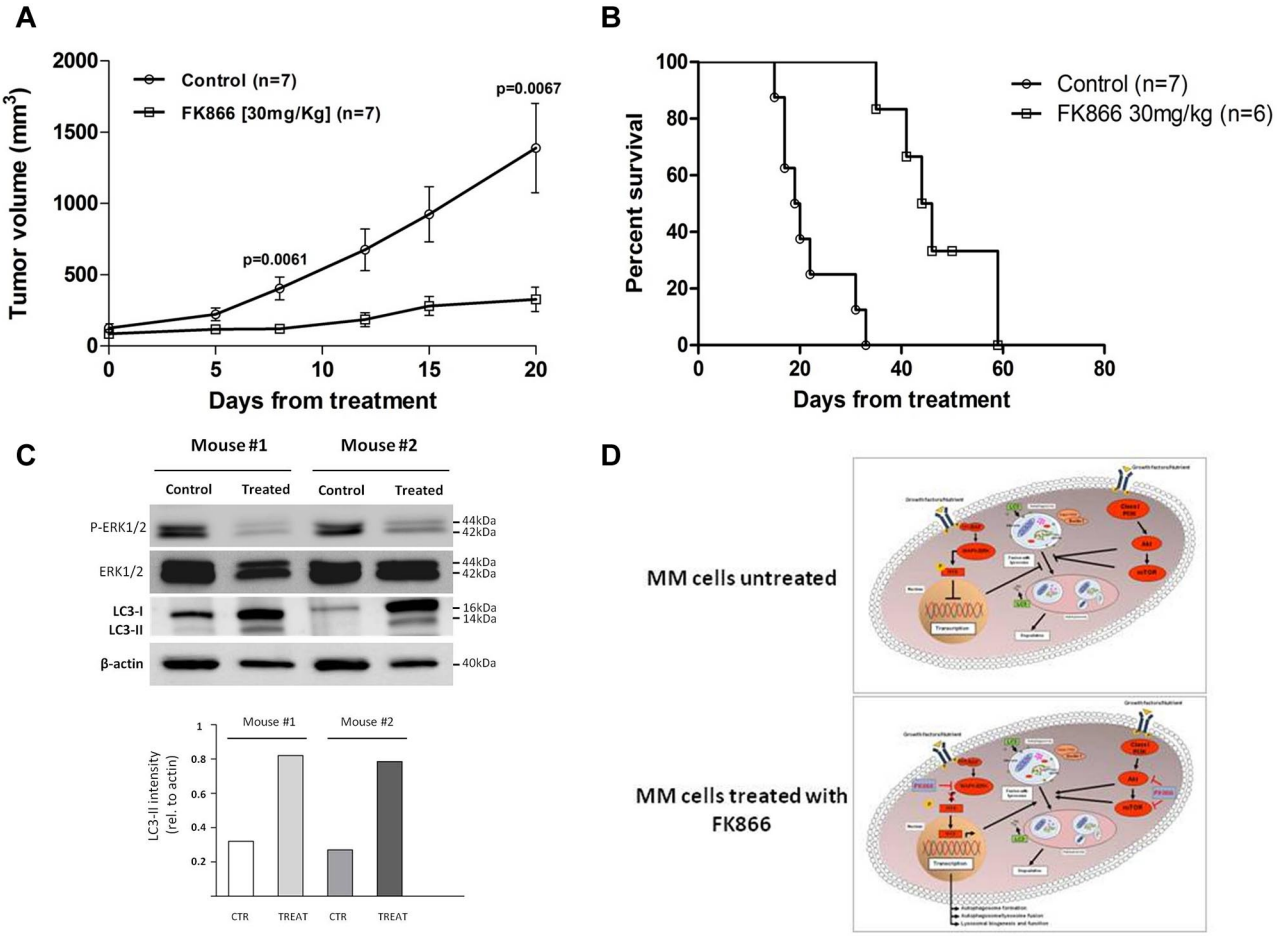

Figure 7. In vivo antimyeloma efficacy of FK866. (A-B) MM.1S cells (3×10^6 in 100 μL of serum free RPMI-1640 medium) were implanted subcutaneously in CB17-SCID mice. After detection of tumor, mice were treated intraperitoneally with FK866 (30 mg/kg body weight) or vehicle twice a day for 4 days in 3 weeks. The treatment significantly inhibited MM tumor growth ($P = .0061$ in the first week and $P = .0067$ at the end of treatment) and increased survival ($P = .0014$) compared with control. Survival was evaluated from the first day of treatment until death using Kaplan-Meier curves. Error bars represent mean ± SD. (C) Tumor tissues from mice treated with vehicle or with FK866 were harvested; whole-tissue lysates were subjected to Western blotting using indicated antibodies. β-actin was used as loading control. Relative intensity of LC3 was calculated by normalizing the LC3-II intensity to β-actin using ImageJ Version 1.46 analysis software. (D) Schematic model of FK866-induced autophagy in MM cells. FK866 inhibits MAPK and induces nuclear translocation of TFEB, thereby up-regulating autophagy-related genes (transcriptional-dependent mechanism), as occurs in starvation conditions. In addition, FK866 directly inhibits PI3K/mTOR activity (nontranscriptional-dependent mechanism), thereby increasing autophagy in MM cells.

results, tumor tissue from FK866-treated mice demonstrated a significant decrease in ERK phosphorylation and proteolytic cleavage of LC3 compared with control. These results establish in vivo proof-of-concept for the investigational study of FK866 in the treatment of MM.

Discussion

Tumor cells exhibit aberrant metabolic activity characterized by high levels of aerobic glycolysis[39] and increased turnover of NAD^+ [40] to support their rapid proliferation. In support of this notion, NAD^+ biosynthesis pathway has recently become a target for innovative therapy.[41,42] Indeed a chemical inhibitor of Nampt induces cell death in several types of human cancers. Importantly, the consequences of Nampt inhibition in healthy PBMCs as well as in $CD34^+$ hematopoietic progenitors[26] are less deleterious, indicating a favorable therapeutic window. Our study identifies for the first time that MM cells are remarkably dependent on Nampt activity for their survival and although proliferating cells are a victim of therapeutic strategies targeting Nampt,[25,26] the almost complete resistance observed in mononuclear cells from MM patients could provide the basis for further clinical investigation of this approach.

We further characterize the downstream effects of therapeutic Nampt inhibition, including autophagic MM cell death. We first show the NAD^+ depletion and cell death in MM cells when Nampt is depleted using either chemical (FK866) or genetic (shRNA-mediated *Nampt* knockdown) methods. We also provide experimental evidence that Nampt inhibition by FK866 overcomes BMSCs, IGF-1, or IL-6–induced MM cell growth. Several recent reports have shown that Nampt inhibition induces cell-death associated with autophagy.[24,29] However, how FK866 induces autophagy is controversial and poorly defined. Here we report different mechanisms whereby intracellular NAD^+ depletion leads to inhibition of cell growth and induction of autophagy in MM cells. Specifically, identification of autophagy as a critical mediator of FK866 cytotoxicity was validated by 4 independent approaches: electron microscopy, proteolytic cleavage of endogenous LC3-I to LC3-II by immunoblotting, formation of LC3 puncta pattern in GFP-LC3–transfected cells, as well as by gene expression profiling. Overall, these findings suggest that a sudden decrease of survival signals

triggered by intracellular NAD^+ depletion induces a rapid increase in autophagy in MM cells.

Given these data, we focused on delineating the molecular events involved in FK866-induced autophagy in MM cells. Specifically, we described 2 mechanisms whereby FK866 triggers autophagy-induced cell death in MM cells.

First, recent studies have shown that dual inhibition of PI3K/mTORC1 activates autophagy[43]; therefore, we examined whether NAD^+ intracellular depletion could affect these signaling cascades. Indeed, FK866 treatment rapidly triggered inhibition of this pathway in MM cells, suggesting that PI3K/mTOR inhibition leads to induction of autophagy. Intracellular NAD^+ shortage observed after FK866 treatment reduces cellular nutrient availability and results in a functional impairment of several cellular functions. As a consequence, pathways depending on cellular energy stores with pivotal roles in MM cell proliferation, such as PI3K/mTOR, might be affected by this event. Also the increased levels of phospho-AKT S473 observed after FK866 treatment (Figure 6A) represent an additional feature indicating dependency on mTORC1 activity,[44] which is also inhibited by treatment with FK866.

Second, gene expression profiling analysis suggested another trigger of autophagy. Specifically, FK866 treatment induced the expression of several autophagy-related genes in MM cells (*ATG9B, ATG4A, ATG4B, ATG16L2, MAPLC3, SQSTM1, UVRAG,* and *WIPI*) independently of mTORC1, providing evidence for mTORC1-independent autophagy. Settembre and colleagues have recently identified a novel transcription-dependent mechanism regulating autophagy,[7] in which transcription factor EB, known to coordinate lysosome formation, functions as an inducer of autophagy when cells are starved. Indeed inhibition of mitogen-activated protein kinase signaling (MAPKs) stimulates the nuclear translocation of TFEB, thereby up-regulating autophagy-related genes. Our results demonstrate that FK866 treatment of MM cells ectopically expressing TFEB (DKK-TFEB) results in nuclear translocation of this transcription factor. We also show that potent MAPK signaling inhibition induced by FK866 results in TFEB nuclear translocation and activation of Atg. Importantly, our microarray data showed a reduction of forkhead box class 'O' (FOXO) 3a proteins after FK866 treatment, providing further evidence of FK866-induced autophagy via a transcription-dependent mechanism. Therefore, we show that anti-MM activity of FK866 is mediated by a transcriptional-dependent (TFEB and FOXO3A) and independent (PI3K/mTORC1) activation of autophagy, which lies upstream of mitochondrial dysfunction and causes cell death. This role of autophagy in mediating FK866 anti-MM activity is novel: FK866 regulates TFEB simultaneously with dual inhibition of PI3K/mTORC1, thereby enhancing autophagy, whereas rapamycin induces autophagy only by suppressing negative regulators (mTORC1). This dual mechanism of FK866 results in increased autophagy and consequent MM cell death (Figure 7D). Although we found no evidence for apoptotic cell death triggered by FK866, it is possible, as proposed by Michallet et al, that the apoptotic program is indeed triggered by Nampt inhibition, but is compromised by the concomitant onset of autophagy.[45] Such an aborted apoptosis could promote the switch from cytoprotective to cytotoxic autophagy. In this context, we hypothesize that ER stress because of intracellular nutrient starvation (NAD^+ shortage) represents the primary mechanism for activating the authophagy death pathway.

Finally, FK866 is well tolerated and significantly inhibited tumor growth in vivo in a murine xenograft MM model. Consistent with our in vitro studies this treatment was associated with features of autophagy, proteolytic cleavage of LC3, as well as ERK1/2 inhibition in tumors harvested from FK866-treated mice. We therefore have identified for the first time a link between intracellular NAD^+ metabolism and autophagy in MM cells, providing the framework developing new targeted therapies in MM.

Acknowledgments

The authors thank the NIMH Chemical Synthesis and Drug Supply Program for generously providing FK866 for this study.

This work was supported by National Institutes of Health (grants RO-1 50947, RO-1 73878), DF/HCC SPORE in Multiple Myeloma (P-50100707); American Italian Cancer Foundation (M.C.); International Multiple Myeloma Foundation and Associazione Cristina Bassi (A.C.); and Associazione Italiana per la Ricerca sul Cancro (START-UP P-6108 A.N.). K.C.A. is an American Cancer Society Clinical Research Professor.

Authorship

Contribution: M.C. and A.C. designed and performed research, analyzed data, and wrote the paper; M.F. and N.M. designed, performed and analyzed animal work; D.C. and T.H. provided input to studies and critically evaluated the paper; Y.-T.T., A.R., A.S., T.C., J.J., S.-Y.K., and F.C. provided reagents and analytic tools; M.G., F.P., A.N. and P. R. provided MM patient samples; and K.C.A. designed the research, critically evaluated, and edited the paper.

Conflict-of-interest disclosure: The authors declare no competing financial interests.

Correspondence: Michele Cea, Dept of Medical Oncology, Dana-Farber Cancer Institute, M551, 450 Brookline Ave, Boston, MA 02115; e-mail: michele_cea@dfci.harvard.edu, or Kenneth C. Anderson, Dana-Farber Cancer Institute, Harvard Medical School, 44 Binney St, Boston, MA 02115; e-mail: kenneth_anderson@dfci.harvard.edu.

References

1. Hallek M, Bergsagel PL, Anderson KC. Multiple myeloma: increasing evidence for a multistep transformation process. *Blood.* 1998;91(1):3-21.
2. Klionsky DJ. Autophagy: from phenomenology to molecular understanding in less than a decade. *Nat Rev Mol Cell Biol.* 2007;8(11):931-937.
3. Levine B, Klionsky DJ. Development by self-digestion: molecular mechanisms and biological functions of autophagy. *Dev Cell.* 2004;6(4):463-477.
4. Levine B. Cell biology: autophagy and cancer. *Nature.* 2007;446(7137):745-747.
5. Efeyan A, Sabatini DM. mTOR and cancer: many loops in one pathway. *Curr Opin Cell Biol.* 2010; 22(2):169-176.
6. Rabinowitz JD, White E. Autophagy and metabolism. *Science.* 2010;330(6009):1344-1348.
7. Settembre C, Di Malta C, Polito VA, et al. TFEB links autophagy to lysosomal biogenesis. *Science.* 2011;332(6036):1429-1433.
8. Zhao J, Brault JJ, Schild A, et al. FoxO3 coordinately activates protein degradation by the autophagic/lysosomal and proteasomal pathways in atrophying muscle cells. *Cell Metab.* 2007;6(6): 472-483.
9. Hideshima T, Bradner JE, Wong J, et al. Small-molecule inhibition of proteasome and aggresome function induces synergistic antitumor activity in multiple myeloma. *Proc Natl Acad Sci U S A.* 2005;102(24):8567-8572.
10. Pan Y, Gao Y, Chen L, et al. Targeting autophagy augments in vitro and in vivo antimyeloma activity of DNA-damaging chemotherapy. *Clin Cancer Res.* 2011;17(10):3248-3258.
11. Chen L, Petrelli R, Felczak K, et al. Nicotinamide

adenine dinucleotide based therapeutics. *Curr Med Chem.* 2008;15(7):650-670.

12. Magni G, Amici A, Emanuelli M, Orsomando G, Raffaelli N, Ruggieri S. Enzymology of NAD+ homeostasis in man. *Cell Mol Life Sci.* 2004; 61(1):19-34.
13. Garten A, Petzold S, Korner A, Imai S, Kiess W. Nampt: linking NAD biology, metabolism and cancer. *Trends Endocrinol Metab.* 2009;20(3):130-138.
14. Revollo JR, Grimm AA, Imai S. The NAD biosynthesis pathway mediated by nicotinamide phosphoribosyltransferase regulates Sir2 activity in mammalian cells. *J Biol Chem.* 2004;279(49): 50754-50763.
15. Rongvaux A, Galli M, Denanglaire S, et al. Nicotinamide phosphoribosyl transferase/pre-B cell colony-enhancing factor/visfatin is required for lymphocyte development and cellular resistance to genotoxic stress. *J Immunol.* 2008;181(7): 4685-4695.
16. Skokowa J, Lan D, Thakur BK, et al. NAMPT is essential for the G-CSF-induced myeloid differentiation via a NAD(+)-sirtuin-1-dependent pathway. *Nat Med.* 2009;15(2):151-158.
17. Nakahata Y, Sahar S, Astarita G, Kaluzova M, Sassone-Corsi P. Circadian control of the NAD+ salvage pathway by CLOCK-SIRT1. *Science.* 2009;324(5927):654-657.
18. Fulco M, Cen Y, Zhao P, et al. Glucose restriction inhibits skeletal myoblast differentiation by activating SIRT1 through AMPK-mediated regulation of Nampt. *Dev Cell.* 2008;14(5):661-673.
19. Van Gool F, Galli M, Gueydan C, et al. Intracellular NAD levels regulate tumor necrosis factor protein synthesis in a sirtuin-dependent manner. *Nat Med.* 2009;15(2):206-210.
20. Belenky P, Bogan KL, Brenner C. NAD+ metabolism in health and disease. *Trends Biochem Sci.* 2007;32(1):12-19.
21. Hasmann M, Schemainda I. FK866, a highly specific noncompetitive inhibitor of nicotinamide phosphoribosyltransferase, represents a novel mechanism for induction of tumor cell apoptosis. *Cancer Res.* 2003;63(21):7436-7442.
22. Wosikowski K, Mattern K, Schemainda I, Hasmann M, Rattel B, Loser R. WK175, a novel antitumor agent, decreases the intracellular nicotinamide adenine dinucleotide concentration and induces the apoptotic cascade in human leukemia cells. *Cancer Res.* 2002;62(4):1057-1062.
23. Wang B, Hasan MK, Alvarado E, Yuan H, Wu H, Chen WY. NAMPT overexpression in prostate cancer and its contribution to tumor cell survival and stress response. *Oncogene.* 2011;30(8):907-921.
24. Nahimana A, Attinger A, Aubry D, et al. The NAD biosynthesis inhibitor APO866 has potent antitumor activity against hematologic malignancies. *Blood.* 2009;113(14):3276-3286.
25. Bruzzone S, Fruscione F, Morando S, et al. Catastrophic NAD+ depletion in activated T lymphocytes through Nampt inhibition reduces demyelination and disability in EAE. *PloS One.* 2009; 4(11):e7897.
26. Cea M, Soncini D, Fruscione F, et al. Synergistic interactions between HDAC and sirtuin inhibitors in human leukemia cells. *PloS One.* 2011;6(7): e22739.
27. Hideshima T, Mitsiades C, Tonon G, Richardson PG, Anderson KC. Understanding multiple myeloma pathogenesis in the bone marrow to identify new therapeutic targets. *Nature Reviews. Cancer.* 2007;7(8):585-598.
28. McMillin DW, Delmore J, Weisberg E, et al. Tumor cell-specific bioluminescence platform to identify stroma-induced changes to anticancer drug activity. *Nat Med.* 2010;16(4):483-489.
29. Billington RA, Genazzani AA, Travelli C, Condorelli F. NAD depletion by FK866 induces autophagy. *Autophagy.* 2008;4(3):385-387.
30. Mizushima N, Yoshimori T, Levine B. Methods in mammalian autophagy research. *Cell.* 2010; 140(3):313-326.
31. Klionsky DJ, Abeliovich H, Agostinis P, et al. Guidelines for the use and interpretation of assays for monitoring autophagy in higher eukaryotes. *Autophagy.* 2008;4(2):151-175.
32. Eng KE, Panas MD, Hedestam GB, Mclnerney GM. A novel quantitative flow cytometry-based assay for autophagy. *Autophagy.* 2010;6(5):634-641.
33. Amaravadi RK, Lippincott-Schwartz J, Yin XM, et al. Principles and current strategies for targeting autophagy for cancer treatment. *Clin Cancer Re.* 2011;17(4):654-666.
34. Jung CH, Ro SH, Cao J, Otto NM, Kim DH. mTOR regulation of autophagy. *FEBS letters.* 2010;584(7):1287-1295.
35. Shi Y, Yan H, Frost P, Gera J, Lichtenstein A. Mammalian target of rapamycin inhibitors activate the AKT kinase in multiple myeloma cells by up-regulating the insulin-like growth factor receptor/insulin receptor substrate-1/phosphatidylinositol 3-kinase cascade. *Mol Cancer Ther.* 2005; 4(10):1533-1540.
36. Cirstea D, Hideshima T, Rodig S, et al. Dual inhibition of akt/mammalian target of rapamycin pathway by nanoparticle albumin-bound-rapamycin and perifosine induces antitumor activity in multiple myeloma. *Mol Cancer Ther.* 2010;9(4):963-975.
37. Chatterjee M, Stuhmer T, Herrmann P, Bommert K, Dorken B, Bargou RC. Combined disruption of both the MEK/ERK and the IL-6R/STAT3 pathways is required to induce apoptosis of multiple myeloma cells in the presence of bone marrow stromal cells. *Blood.* 2004;104(12):3712-3721.
38. Hideshima T, Anderson KC. Molecular mechanisms of novel therapeutic approaches for multiple myeloma. *Nat Rev Cancer.* 2002;2(12):927-937.
39. Warburg O. On the origin of cancer cells. *Science.* 1956;123(3191):309-314.
40. Khan JA, Forouhar F, Tao X, Tong L. Nicotinamide adenine dinucleotide metabolism as an attractive target for drug discovery. *Expert Opin Ther Targets.* 2007;11(5):695-705.
41. Ziegler M. New functions of a long-known molecule. Emerging roles of NAD in cellular signaling. *Eur J Biochem.* 2000;267(6):1550-1564.
42. Jacobson MK, Twehous D, Hurley LH. Depletion of nicotinamide adenine dinucleotide in normal and xeroderma pigmentosum fibroblast cells by the antitumor drug CC-1065. *Biochem.* 1986; 25(20):5929-5932.
43. Degtyarev M, De Maziere A, Orr C, et al. Akt inhibition promotes autophagy and sensitizes PTEN-null tumors to lysosomotropic agents. *J Cell Biol.* 2008;183(1):101-116.
44. Boulay A, Lane HA. The mammalian target of rapamycin kinase and tumor growth inhibition. *Recent Results Cancer Res.* 2007;172:99-124.
45. Michallet AS, Mondiere P, Taillardet M, Leverrier Y, Genestier L, Defrance T. Compromising the unfolded protein response induces autophagy-mediated cell death in multiple myeloma cells. *PloS One.* 2011; 6(10):e25820.